Complementary actions of dopamine D2 receptor 1 agonist and anti-Vegf therapy on tumoral vessel normalization in a transgenic mouse model

Title: Complementary actions of dopamine D2 receptor agonist and anti-Vegf therapy on tumoral vessel normalization in a transgenic mouse model

Short Title: Tumoral vessel normalization by dopamine and Vegf blockade

Authors: Norbert Chauvet[1,2,3,$], Nicola Romanò[1,2,3,$$], Chrystel Lafont[1,2,3], Anne Guillou[1,2,3], Evelyne Galibert[1,2,3], Xavier Bonnefont[1,2,3], Paul Le Tissier[4], Monica Fedele[5], Alfredo Fusco[5], Patrice Mollard[1,2,3] and Nathalie Coutry[1,2,3].

[1] CNRS, UMR-5203, Institut de Génomique Fonctionnelle, Montpellier, F-34094, France

[2] INSERM, U1191, Montpellier, F-34094, France

[3] Université de Montpellier, UMR-5203, Montpellier, F-34094, France.

[4] Centre for Integrative Physiology, University of Edinburgh, Edinburgh, EH8 9XD, United Kingdom.

[5] Istituto di Endocrinologia ed Oncologia Sperimentale del CNR e/o Dipartimento di Medicina Molecolare e Biotecnologie Mediche, Università degli Studi di Napoli "Federico II", 80131 Naples, Italy.

$ Present address: PhyMedExp, INSERM U1046, CNRS UMR-9214, Université de Montpellier, 34295 Montpellier Cedex 5, France.

$$ Present address: Centre for Integrative Physiology, University of Edinburgh, Edinburgh, EH8 9XD, United Kingdom.

Corresponding author: Nathalie Coutry, Institut de Génomique Fonctionnelle, 141 rue de la Cardonille, 34094 Montpellier CEDEX 05, France. Nathalie.Coutry@igf.cnrs.fr.

Keywords: Angiogenesis, mouse model, pituitary adenomas, combination therapy, GPCR ligand.

Abbreviations: D2R, Dopamine Receptor D2; GPCRs, G Protein-Coupled Receptors; DA, Dopamine; PRL, Prolactin; WT, Wild-Type; TH, Tyrosine Hydroxylase; pTH, Phosphorylated Tyrosine Hydroxylase; TEM, Transmission Electron Microscopy; SEM, Scanning Electron Microscopy; TIDA neurons, TuberoInfundibular Dopamine Neurons.

Article Category: Research Article - Cancer Therapy and Prevention

Novelty and Impact: Angiogenesis in tumors favors many aspects of disease development and compromises treatment efficiency. The authors aimed to identify a treatment to normalize tumoral vessels and restore normal blood perfusion with a Vegf receptor inhibitor and/or a ligand of dopamine G protein-coupled receptor D2. These findings offer a preclinical proof of concept for a combination therapy that exhibits a robust efficacy to abrogate intratumoral hemorrhage and restores blood vessel perfusion in a mouse model of prolactinoma.

Financial support: This work was supported by grants from Institut National de la Santé et de la Recherche Médicale; Centre National de la Recherche Scientifique; Université de

Montpellier; the Agence Nationale de la Recherche (ANR-2010-BLAN-1415-01 and ANR 12 BSV1 0032-01) and the Cancéropôle Grand Sud-Ouest.

Conflict of interest: The authors disclose no potential conflicts of interest.

Abstract

Angiogenesis contributes in multiple ways to disease progression in tumors and reduces treatment efficiency. Molecular therapies targeting Vegf signaling combined with chemotherapy or other drugs exhibit promising results to improve efficacy of treatment. Dopamine has been recently proposed to be a novel safe antiangiogenic drug that stabilizes abnormal blood vessels and increases therapeutic efficacy. Here, we aimed to identify a treatment to normalize tumoral vessels and restore normal blood perfusion in tumor tissue with a Vegf receptor inhibitor and/or a ligand of dopamine G protein-coupled receptor D2 (D2R). Dopamine, via its action on D2R, is an endogenous effector of the pituitary gland, and we took advantage of this system to address this question. We have used a previously described Hmga2/T mouse model developing haemorrhagic prolactin-secreting adenomas. In mutant mice, blood vessels are profoundly altered in tumors, and an aberrant arterial vascularization develops leading to the loss of dopamine supply. D2R agonist treatment blocks tumor growth, induces regression of the aberrant blood supply and normalizes blood vessels. A chronic treatment is able to restore the altered balance between pro- and anti-angiogenic factors. Remarkably, an acute treatment induces an up-regulation of the stabilizing factor Angiopoietin 1. An anti-Vegf therapy is also effective to restrain tumor growth and improves vascular remodeling. Importantly, only the combination treatment suppresses intratumoral hemorrhage and restores blood vessel perfusion, suggesting that it might represent an attractive therapy targeting tumor vasculature. Similar strategies targeting other ligands of GPCRs involved in angiogenesis may identify novel therapeutic opportunities for cancer.

Introduction

Pathological angiogenesis, generated by an imbalance of pro- and antiangiogenic factors, provides oxygen and nutrients to tumors, and is a hallmark of many benign and malignant diseases [1, 2]. New blood vessels within tumors are impaired in their function and structure, and this abnormal vascular network causes alterations in blood flow and oxygenation that can further increase tumor growth and alter the anti-tumor efficiency of cytotoxic drugs [3, 4]. Results from clinical trials using anti-Vegf agents have revealed that efficacy of anti-angiogenic monotherapy can be inadequate in term of response or survival rates [5]. To improve treatment efficiency, novel combinations of anti-Vegf therapy with chemotherapy or radiation have been developed, with promising results [5, 6]. Thus, a recent study performed by Jain's group investigating a combination treatment with anti-Vegf and chemotherapy, showed that early vessel normalization improves tumor perfusion and survival in a subset of glioblastoma patients [7]. Of interest, another option is to combine Vegf-signaling inhibitors with antiangiogenic agents targeting alternative pathways. In this regard, the use of inhibitors targeting Vegf and Angiopoietin 2 has shown complementary actions on tumor growth and angiogenesis [8, 9].

Alternative strategies for normalizing vessels and blood flow in tumoral tissues are based on the use of ligands for G protein-coupled receptors (GPCRs) [10]. Among the recently discovered candidates, D2 receptors and their natural ligand dopamine (DA) are of particular interest as, in addition to its major role as a neurotransmitter within the brain, DA controls vascular tone and blocks Vegf-dependent increase in vascular permeability [11, 12]. DA influences tumor behavior as well, especially by controlling cell proliferation and processes leading to angiogenesis [13, 14]. DA is not only an anti-tumoral and anti-angiogenic drug, it also normalizes abnormal tumor blood vessels by acting on pericytes and endothelial cells, and therefore improves tumor perfusion by increasing blood flow, decreasing hypoxia and

enhancing the concentration of anti-cancer drug in tissue [15]. A recent study showed that DA therapy also prevents 5-fluoracil mediated neutropenia [16]. Hence, DA has been proposed to be a novel therapy for the treatment of cancer and chemotherapy-induced disorders [15-17].

In this context, we examined whether an anti-Vegf therapy combined with D2 receptor ligands could exert additive effects to normalize blood vessels in tumors. We tested this hypothesis on the pituitary gland since DA is also an endogenous effector of this master gland and plays a central role in tonically inhibiting prolactin (PRL) release via D2 receptors located on lactotrophs [18]. Blood perfuses the normal pituitary via incoming vessels from the pituitary portal circulation at the base of the brain. Previous studies have reported that prolactinomas in rats [19] and in humans [20] are associated with the development of a direct arterial blood supply, which may lead in turn to an escape from inhibitory hypothalamic regulation since systemic blood contains very low DA levels in comparison with portal blood. Prolactinomas are in general treated by medical therapy with DA agonists, and an anti-angiogenic strategy using anti-Vegf agents has been recently proposed to treat aggressive human pituitary tumors [21]. These tumors are therefore an excellent model for investigation of the use of DA and Vegf for tumor therapy through modification of vascular defects.

We have used the Hmga2/T mouse model, which develops PRL-secreting adenomas [22] and has been previously used to test the efficacy of new drugs for the therapy of human pituitary tumors [23], to investigate the status of endogenous DA during tumoral development and the effects of a D2R agonist on tumor growth and vasculature. Moreover, we have examined whether DA and anti-Vegf agent could exert complementary effects on structural and functional properties of tumoral blood vessels. We show that a loss in endogenous DA inhibitory tone is concomitant with tumor progression and is associated with aberrant growth of blood vessels. D2R agonist treatment inhibits tumor growth and normalizes abnormal blood vessels. Molecular mechanisms induced by D2R agonist are able to reverse the

profound alterations of the angiogenic profile in tumoral glands and involve an up-regulation of the stabilizing factor Angiopoietin1. Strikingly, although anti-Vegf treatment is also able to normalize tumoral blood vessels and prevents tumor growth, only the combination treatment suppresses intratumoral hemorrhage and restores blood vessel perfusion.

Materials and Methods

Mouse model

All animal studies complied with the animal welfare guidelines of the European Community. They were approved by the Direction of Veterinary departments of Herault and the Languedoc Roussillon Institutional Animal Care and Use Committee (#CEEA-LR-12119). Animals were housed in light (12-hour light, 12-hour dark cycle) and temperature (22-24°C) controlled rooms and fed a normal diet with free access to tap water.

Experiments were performed on mixed 129/SVJ x C57BL/6 female mice, either wild-type (WT) or overexpressing ubiquitously a truncated form of Hmga2 protein [24] (Hmga2/T mice). In this model, pituitaries from females exhibited an extended period of hyperplasia, starting around 3 months of age, followed by tumor onset between 9 to 11 months (Supporting Information Fig. 1). These tumors appeared very hemorrhagic and immunohistochemical experiments showed that they were prolactinomas. A strong correlation was observed between circulating PRL levels and tumor weight ($R^2 = 0.936$), as reported in human prolactinomas [25, 26]. We thus decided to monitor hormone output for each mouse once a week to follow tumor initiation and progression. Unless otherwise specified, the majority of experiments were performed on cohorts of mice with circulating PRL concentrations between 400 and 800 ng/ml and corresponding to tumors of 13-18 mg.

ELISA assay for PRL

Blood levels of PRL were measured using an ultra-sensitive ELISA method recently established in the laboratory [27]. Briefly, whole blood (4 µl) was collected from the tail vein of conscious mice, immediately diluted (1/30) in PBS-T (PBS, 0.05% Tween20), and then frozen at –20°C until use.

Injection or administration of drugs in mice

The dopaminergic inhibitory tone was evaluated by an intraperitoneal (ip) injection of the D2R antagonist domperidone (20 mg/kg, Abcam) and measurement of circulating PRL 3 times before (basal) and then 30 min and 45 min after the injection. The DA inhibitory tone was determined by the maximum fold increase in PRL blood levels and corresponds to the ratio between the maximum secretion and the basal level (mean of PRL blood concentration of the 3 points preceding domperidone injection).

Bromocriptine mesylate implants (60 days, 10 mg pellet, Innovative Research of America) were placed under the skin of the neck of Hmga2/T mice harboring pituitary tumors, for 6 weeks. Some mice received ip injections of bromocriptine (6 mg/kg, Sigma-Aldrich) twice a day over the course of 48 h.

Axitinib (20 mg/kg, Abmole Bioscience Inc.) or sucralose were given to the mice by voluntary oral administration, twice a day for 6 weeks, after training of the mice (http://www.nature.com/protocolexchange/protocols/2099).

Immunohistochemistry

Immunohistochemical analyses were performed as previously reported [28]. Briefly, pituitary tissue sections from WT and Hmga2/T mice with and without various treatments were prepared with a vibratome and then stained with a sheep polyclonal tyrosine hydroxylase antibody (TH, 1:1000, Ab113, Abcam), with a rabbit polyclonal phosphorylated

TH antibody (pTH, 1:1000, AB5423, Milipore), or with a rat monoclonal endomucin antibody (1:500, sc-53941, Santa Cruz) as a marker for pituitary endothelial cells. In one set of experiments, pituitary paraffin sections were stained with a rat monoclonal endomucin antibody (1:500, sc-53941, Santa Cruz). Sections were observed with an epifluorescence (Carl-Zeiss Axio Imager Z1) or a confocal microscope (LSM510 Zeiss). Four parameters were evaluated using ImageJ software to characterize quantitatively pituitary microvasculature: the mean vessel area, the microvessel density, the total vessel area and the area of extravasation of red blood cells. Detailed protocol is presented in Supporting Information Material and Method section.

Scanning and Transmission Electron Microscopy

Ultrastructural analyses were performed as previously described [29], in WT and Hmga2/T mice receiving or not different treatments. Different parameters characterizing blood vessel structure observed by Transmission Electron Microscopy (TEM) were quantified using ImageJ software: the perimeter of the lumen, the circularity (a value of 1 indicates a perfect circle) and the solidity (defined as the ratio of an object area/area of the convex hull of the object, objects with irregular shapes have a solidity value approaching 0), reflecting the tortuosity of the vessels.

Injection of microspheres in the general circulation

To assess vascular supply in pituitary adenomas, fluorescent microsphere were injected in the circulation following a previously described protocol [19]. Minor modifications are presented in Supporting Information Material and Methods section.

***In vivo* amperometry**

A detailed protocol of *in vivo* amperometry is given in Supporting Information Material and Methods section. Briefly, after anaesthesia with ketamine-xylazine, mice were fixed on a stereotactic frame, and a carbon fiber microelectrode was inserted in a support guide cannula, with its tip reaching the median eminence at stereotaxic coordinates -1.3 mm rostro-caudal; 0 mm medio-lateral; 6.1 mm ventral. After at least one week of recovery, mice were transferred to the recording cages and connected to an electrical swivel to enable free movement. The microelectrodes were maintained at 700 mV to detect secretion of DA, and oxidation currents were recorded at 1 kHz.

In vivo imaging of pituitary gland

Cellular *in vivo* imaging of the pituitary gland allows determination of microvascular organisation and blood flow in the same region of the gland, and a detailed protocol has been previously reported [30]. Injections of 150 kDa FITC-labeled dextran (Sigma-Aldrich) were performed via the jugular vein in WT and Hmga2/T mice. Fluorescence emission was captured by an EM-CCD camera 512 x 512 C9100 (Hamamatsu) and acquired with MetaMorph software (Molecular Devices).

Blood vessel perfusion

WT or Hmga2/T mice were anesthetized by inhalation of isoflurane (1.5% in O_2) and a catheter was inserted in the jugular vein. Perfusion of blood vessels was evaluated after an intravenous injection of 1 mg of fluorescent 500 kDa dextran (dextran fluorescein, lysine fixable, Molecular Probes). After circulation for 15 min, a thoracic lethal dose of pentobarbital was administrated to the mice and pituitaries were fixed in 4% PFA. Tissue sections were prepared using a vibratome, and blood vessels were immunostained using an

endomucin antibody. Volocity software was used to measure overlap coefficient (M1) according to Manders et al. [31] reflecting the portion of blood vessels filled with dextran.

Real-time RT-PCR

Adenohypophysis were dissected from terminally anaesthetized mice. Total RNA was extracted and then reverse-transcribed as previously described [28, 32]. Specific primers for qRT-PCR were designed using the Primer Express 3.0 software, the sequences are shown in Supporting Information Table 1. PCR reactions are presented in Supporting Information Material and Method section.

Statistics

Values represent mean ± SEM. Statistical tests were performed with Prism (GraphPad software). Normality was assessed using D'Agostino-Pearson test. Non-parametric statistical tests were used for some data sets, as indicated in figure legends. Multiple comparisons tests were selected when the number of data sets were >2. Statistical difference between groups was assumed when $P<0.05$.

Results

Aberrant blood supply leads to loss of dopaminergic inhibitory tone, associated with tumor progression

We first characterized the vascular network in pituitary tumors by immunohistochemistry, scanning electron microscopy (SEM) and TEM (Fig. 1). The results demonstrate remodeling of the microvasculature in the tumors and structural abnormalities. The vascular density was decreased in tumors compared to WT, and tumoral blood vessels were dilated, tortuous and structurally altered (Fig. 1A and B) since blood lakes were present

(Fig. 1B and J). Changes in the organization of the vascular architecture in tumors were also confirmed at the ultrastructural level (Fig. 1 C to J). The endothelium of the blood vessels was irregular, discontinuous and damaged, presenting numerous protrusions into the lumen of the vessels, as described for other tumor types [33].

To test whether tumorigenesis in our model was associated with the development of a direct arterial blood supply, we injected in the systemic circulation fluorescent microspheres with a diameter which is too large to pass through the primary portal capillaries in the median eminence (Supporting Information Fig. 2). Whilst in WT animals microspheres were restricted to the median eminence (Supporting Information Fig. 2A and B), in mice harboring tumors microspheres were also localized in the tumoral region (Supporting Information Fig. 2C and D). The development of such an aberrant growth of blood vessels in tumors was directly visualized by *in vivo* imaging of the pituitary after an intravenous injection of fluorescent dextran. In WT mice (Fig. 1K), as expected, blood flow arrived from the median eminence through the portal system, and filled capillaries from the entire gland in a rostro-caudal direction in less than 30 s. Although arteries from meninges surrounding pituitary were rapidly filled (t = 2 s), they never branched with the adenohypophysis blood vessels. By contrast, in Hmga2/T mice with a tumor beginning to develop (Fig. 1L), the blood flow from the portal system in the hyperplastic area was strongly slowed, while the tumoral region was perfused by vessels derived from dural arteries (Fig. 1L, arrow heads).

The development of this aberrant direct vascularization induced a loss of endogenous DA inhibitory tone, although DA was still produced and released by tuberoinfundibular dopamine (TIDA) neurons (Fig. 2). By determining circulating PRL after an injection of a D2R antagonist, domperidone, in WT and hyperplastic glands, we found that the endogenous DA inhibitory tone was high (Fig. 2A). By contrast, it was decreased in 7-20 mg tumors, and very low, albeit still present, in tumors ≥ 20 mg. In addition, phosphorylated tyrosine

hydroxylase (the key enzyme involved in DA synthesis) was still present in neurons from the arcuate nucleus from Hmga2/T mice with pituitary tumors (Fig. 2B), suggesting that DA was produced in TIDA neurons. Accordingly, DA was released *in vivo* by TIDA neurons in the median eminence where it normally diffuses into the capillaries of the pituitary portal blood vessels. We performed *in vivo* amperometric measurements of DA secretion (Fig. 2C). Episodic secretion of DA was still detectable in animals with pituitary tumors, and did not appear grossly different from that in WT animals (Nicola Romanò, personal communication). Furthermore, the frequency of amperometric events did not decrease during tumor development (Fig 2C).

Overall, these findings show that establishment of an aberrant blood supply leads to the loss in DA inhibitory tone, secondary to tumor onset, without major hypothalamic dysfunction.

D2R agonist blocks aberrant blood supply, tumor progression and restores angiogenic balance

To evaluate the impact of restoring DA on blood supply, we treated mice harboring pituitary tumors (Tumors t0), with subcutaneous implants of a D2R agonist bromocriptine for 6 weeks (Bromocriptine 6 wks), and then analyzed the presence of the aberrant growth of blood vessels (Fig. 3). Of note, bromocriptine was able to inhibit PRL secretion: 24 hours after the implantation circulating PRL concentrations were low and remained controlled until sacrifice (< 50 ng/ml, data not shown), indicating that the Hmga2/T model had the ability to respond to bromocriptine treatment. This treatment totally blocked tumoral growth compared to untreated tumors (Tumors 6 wks, Fig. 3B). Pituitary weight was similar to that measured in Tumors t0 (Fig. 3B), and pituitaries appeared less hemorrhagic (Fig. 3A). Strikingly, bromocriptine treatment inhibited the progression of the aberrant vascularization as revealed

by a drastic decrease in the number of microspheres in pituitaries from bromocriptine-treated animals compared to untreated mice (Fig. 3C). The 5-fold decrease in the number of microspheres quantified between Tumors t0 and bromocriptine-treated tumors suggests that the D2R agonist induced a partial regression of the pre-existing aberrant vascularization. Immunostaining for D2R showed that D2R was present as expected in lactotrophs, but it was also detected in pituitary blood vessels (Supporting Information Fig. 3), suggesting that DA could exert its effects directly on blood vessels.

We then investigated whether this chronic D2R agonist treatment could affect the expression of a panel of pro- and anti-angiogenic factors. Fig. 3D shows that the angiogenic profile, assessed by qPCR, was affected in tumors: angiogenic factor expression was up- or down-regulated, whilst during the period of hyperplasia, modulations were modest (Supporting Information Fig. 4A). Interestingly, bromocriptine treatment for 6 weeks was able to reverse these alterations (Fig. 3E) and restored an angiogenic signature close to that observed during hyperplasia (Supporting Information Fig. 4B).

We next assessed the kinetics of bromocripine action on the angiogenic gene expression profile. After 2 days of treatment, among the set of genes studied, only 2 were rapidly regulated by bromocriptine (Fig. 3F; Supporting Information Fig. 4C): *angiopoietin 1* (*Angpt1*) and *Prok1* (also named EG-Vegf) an angiogenic mitogen specific to endocrine glands [34]. The mRNA levels for *Angpt1* were low in tumors and an acute bromocriptine treatment restored its expression totally since the mRNA levels were similar to that found in WT animals (relative expression for *Angpt1*: 2.37 ± 0.32 in WT vs 2.41 ± 0.47 in bromocriptine-treated mice). *Prok1* expression was partially restored by an acute bromocriptine treatment: relative expression for *Prok1* was 1.68 ± 0.13 and 0.98 ± 0.46 in WT and bromocriptine-treated mice, respectively. *Vegfa* expression was not affected by bromocriptine treatment. Altogether, these results show that the D2R agonist blocked tumor

growth, induced regression of the aberrant vascularization and up-regulated the expression of *Angpt1* and *Prok1*.

Vegf contributes both to aberrant blood supply and tumoral growth

Vegf has been shown to be involved in normal and tumoral vascular remodeling [5, 35] and has been reported to contribute to pituitary tumor progression in a murine model [36]. We investigated whether Vegf could participate in the occurrence and development of the aberrant vascularization in tumors. We first established that aberrant direct vascularization starts to develop in mice with circulating PRL between 75 and 100 ng/ml (data not shown). We treated mice exhibiting such concentrations of PRL for 6 weeks with axitinib, a potent inhibitor of tyrosine kinase and selective from VegfR [37]. Axitinib-treated tumors appeared less hemorrhagic than control tumors (Fig. 4A) and the antiangiogenic agent partially blocked tumor progression (Fig. 4B). The number of microspheres quantified in axitinib-treated tumors was significantly lower than in those of controls, demonstrating that Vegf contributes to the establishment of the aberrant blood supply in tumors (Fig. 4C). The effects of axitinib on expression of pro- and anti-angiogenic factors (Fig. 4D) showed that the angiogenic gene profile was differentially affected by axitinib compared to bromocriptine treatment (Fig. 3E), although some genes were regulated in a similar way by both treatments such as *Rgs5* and *Cspg4* for example. Importantly, the expression of *Angpt1* and *Prok1*, which was up-regulated in response to bromocriptine treatment, was unchanged and remained low after axitinib treatment (Fig. 4D). These results suggest that D2R agonist treatment and anti-Vegf therapy could involve common as well as independent effects on angiogenic pathways.

Bromocriptine or axitinib correct the structural abnormalities of tumoral vessels while the combination treatment restores blood vessel perfusion

We further addressed the complementary effects of D2R agonist and anti-Vegf therapy on blood vessel normalization (Fig. 5 and Supporting Information Fig. 5). Figure 5A shows that the combination treatment greatly reduced intratumoral hemorrhage. Analysis of pituitary vasculature in various conditions and morphometric measurements of blood vessels demonstrate that D2R agonist or axitinib had an equivalent capacity to improve structural defects present in tumoral blood vessels and that the combination treatment did not lead to a significant advantage (Fig. 5B and C and Supporting Information Fig. 5). Whilst vascular density was maintained in presence of D2R agonist treatment compared to untreated-tumors, axitinib notably decreased vascular density. In addition, blood vessel dilatation and tortuosity were improved by the different treatments (Supporting Information Fig. 5).

Leakiness of tumoral blood vessels is of particular functional significance and intratumoral hemorrhage constitutes an indicator of this leakiness [33]. Importantly, the combination treatment dramatically reduced leakiness of blood vessels (Fig. 5D). Quantification of the area of extravasation in various conditions showed that intratumoral hemorrhage in tumors represented more than 7% of the total surface area. Although it was significantly reduced by both bromocriptine or axitinib, only the combination treatment was able to prevent vessel leakiness since intratumoral hemorrhage was almost absent in bromocriptine + axitinib-treated tumors.

Because of the highly disorganized epithelium lining endothelial cells, blood vessel perfusion is severely impaired in tumors [38]. We assessed whether the positive effects of the combination treatment also included an improved vessel perfusion (Fig. 6). The portion of blood vessels filled with FITC-dextran was significantly decreased in tumors compared to WT (Fig. 6A and B), indicating that perfusion within the tumors was strongly affected and inappropriate. Bromocriptine- and axitinib-treatment improved partially vessel perfusion, and the combination treatment restored this almost entirely. Together, these results show that,

whilst bromocriptine and/or axitinib were able to correct structural abnormalities of tumoral vessels with a similar efficacy, only the combination treatment restored their function.

Discussion

We report here that a combination of D2R agonist treatment with anti-Vegf therapy specifically suppresses intratumoral hemorrhage and restores the perfusion of blood vessels. PRL-secreting pituitary adenomas undergo profound vascular remodeling along with formation of an aberrant arterial blood supply resulting in an escape from inhibitory hypothalamic regulation by DA. D2R agonist treatment blocks tumor growth and remarkably ameliorates abnormal blood vessel function. In addition, the altered balance between pro- and anti-angiogenic factors in tumors is restored by D2R agonist administration. An anti-Vegf therapy is also able to inhibit tumor growth and improves vascular remodeling. Furthermore, we show for the first time that a combination of anti-Vegf and GPCR ligand therapy exerts complementary effects on tumoral blood vessel normalization.

Dual effects of dopamine on angiogenesis process. We show, in accordance with previous studies [35, 36], that anti-Vegf therapy induced a drastic reduction in vascular density. This anti-angiogenic effect was effective both on capillaries of the portal system and the extra-portal aberrant vascularization. By contrast, D2R agonist effects specifically induced the regression of the extra-portal aberrant vascularization. These antiangiogenic effects might be mediated in part via DA action on Vegf signaling [11, 39, 40]. Notably, both treatments strongly down-regulated the angiogenic factor Rgs5, whose expression is closely associated with tumor-induced neovascularization and drastically reduced in vessels normalized under therapy [41]. Despite the regression of this extra-portal blood system, the maintenance of the vascular density in D2R agonist-treated tumors may be due to the formation of *de novo* capillaries derived from the portal system, suggesting that DA could exert dual effects on

vascularization. Endothelial cells display a strong heterogeneity in terms of structure, function or gene expression [42]. It is now well established that in tumors endothelial cells show multiple phenotypes that can vary during tumor progression and are mainly determined by the microenvironment [43]. It is possible that D2R agonists act on both the extraportal and the portal blood system by distinct mechanisms, and these effects are probably mediated via different combinations of effectors. In this respect, Prok1 (also named EG-Vegf) is an interesting candidate to mediate specific DA actions. In humans, Prok1 has been shown to have a highly tissue-specific pattern of expression, and was proposed to be a mitogen that could regulate tissue-specific proliferation and differentiation of endothelial cells [34], in particular in endocrine glands. We show that its expression is down-regulated in prolactinomas and rapidly restored by D2R agonist treatment. Thus, this angiogenic factor could play a role in DA-induced vasculature remodeling, especially in the formation of *de novo* blood vessels from the portal system.

Vascular normalization by D2R agonist and Vegf inhibition. Although anti-Vegf specific monotherapy may not be as effective as initially expected in term of response and increase survival in patients with cancers, its combination with modulation of other signaling pathways may have promise [5, 6]. We show that anti-Vegf and D2R agonist treatments given alone displayed partial and similar efficiency on blood vessel perfusion and intratumoral hemorrhage. Remarkably, D2R agonist and blockade of Vegf together had additive effects on vascular perfusion and leakage, suggesting complementary modes of action. This is supported by analysis of angiogenic factors rapidly regulated by DA, which highlighted Angpt1 as a putative candidate normalizing blood vessels. Up-regulation of Angpt1 was also maintained during long term D2R agonist treatment, while after anti-Vegf monotherapy Angpt1 levels remained low. Angpt1 and 2 are ligands of the vascular endothelial Tie2 receptor and bind to Tie2 with similar affinities, however they behave as mutual antagonists [44]. Therefore, the

425 balance of Angpt1 and Angpt2 is critical for control of vascular normalization or angiogenesis
426 via the same Tie2 receptor [45]. Of note, in the present study, the Angpt1/Angpt2 ratio was
427 decreased in tumors, and this ratio was reversed with the administration of D2R agonists.
428 Vegf and Angpt1 exert antagonist effects on endothelial barrier function since Vegf increases
429 vascular permeability, an effect which is inhibited by Angpt1, which also promotes blood
430 vessels stabilization [44]. Recent studies show that targeted Angpt1 monotherapy in pathological
431 conditions is highly effective to suppress vascular leakage [46, 47]. Moreover, DA-normalization
432 of blood vessels in murine orthotopic models of colon and prostate cancers involved up-
433 regulation of Angpt1 [15]. We show here that DA effects on Vegf signaling is not sufficient to
434 abrogate vascular leakage and concomitant Vegf blockade is required to totally suppress
435 intratumoral hemorrhage.

436 In summary, the present study demonstrates that D2R agonist and anti-Vegf therapy
437 exert complementary actions on tumoral vessel normalization. This combinatorial approach
438 might constitute an interesting option in treatment of prolactinomas, especially in cases where
439 current therapy is ineffective or poorly tolerated. We anticipate that the novel combination
440 treatment proposed in the present study could treat different tumor types in which DA exerts
441 anti-angiogenic effects or normalizes tumoral blood vessels, such as ovarian carcinoma, lung
442 cancer or colon cancer [15, 16, 48, 49]. Growing evidence implicates GPCRs and their downstream
443 signaling pathways in cancer pathology, especially angiogenesis [50]. Since the GPCRs are
444 excellent drug targets, a similar combinatorial strategy extending to different ligands of
445 GPCRs involved in angiogenesis may identify novel therapeutic opportunities for cancer.
446

447 ## Acknowledgments

448 The authors would like to thank J. Guillemin and F. Gallardo from animal facility of Institute
449 for Functional Genomics for their assistance with the transgenic mouse lines, and are grateful

to S. Debiesse for genotyping service. Dr A. O. Martin is gratefully acknowledged for helpful discussions on the project, Dr P. de Santa Barbara for critical reading of the manuscript, and P. Fontanaud for technical assistance with imaging analysis. The authors thank Dr C. Cazevieille for assistance with the electron microscope (Montpellier RIO Imaging-INM-COMET).

Statement of author contributions

NC, NR, CL and NC conceived, designed and carried out experiments. Data were analysed and interpreted by NC, NR, CL and NC. NC and NC supervised the project. AG and EG carried out experiments. MF and AF provided the Hmga2/T mouse model. NC, NR, XB, PLT, PM and NC were involved in writing the manuscript. All authors had final approval of the manuscript.

References

1. Carmeliet P, Jain RK. Molecular mechanisms and clinical applications of angiogenesis. Nature 2011;473:298-307.

2. Goel S, Duda DG, Xu L, Munn LL, Boucher Y, Fukumura D, Jain RK. Normalization of the vasculature for treatment of cancer and other diseases. Physiol Rev 2011;91:1071-121.

3. Hanahan D, Folkman J. Patterns and emerging mechanisms of the angiogenic switch during tumorigenesis. Cell 1996;86:353-64.

4. Jain RK. Normalization of tumor vasculature: an emerging concept in antiangiogenic therapy. Science (New York, N.Y.) 2005;307:58-62.

5. Jain RK, Duda DG, Clark JW, Loeffler JS. Lessons from phase III clinical trials on anti-VEGF therapy for cancer. Nat Clin Prac Oncol 2006;3:24-40.

6. Jayson GC, Kerbel R, Ellis LM, Harris AL. Antiangiogenic therapy in oncology: current status and future directions. Lancet 2016.

7. Batchelor TT, Gerstner ER, Emblem KE, Duda DG, Kalpathy-Cramer J, Snuderl M, Ancukiewicz M, Polaskova P, Pinho MC, Jennings D, Plotkin SR, Chi AS, et al. Improved tumor oxygenation and survival in glioblastoma patients who show increased blood perfusion after cediranib and chemoradiation. Proc Natl Acad Sci USA 2013;110:19059-64.

8. Hashizume H, Falcon BL, Kuroda T, Baluk P, Coxon A, Yu D, Bready JV, Oliner JD, McDonald DM. Complementary Actions of Inhibitors of Angiopoietin-2 and VEGF on Tumor Angiogenesis and Growth. Cancer Res 2010;70:2213-23.

9. Peterson TE, Kirkpatrick ND, Huang YH, Farrar CT, Marijt KA, Kloepper J, Datta M, Amoozgar Z, Seano G, Jung K, Kamoun WS, Vardam T, et al. Dual inhibition of Ang-2

and VEGF receptors normalizes tumor vasculature and prolongs survival in glioblastoma by altering macrophages. Proc Natl Acad Sci USA 2016;113:4470-75.

10. Lappano R, Maggiolini M. G protein-coupled receptors: novel targets for drug discovery in cancer. Nat Rev Drug Discov 2011;10:47-60.

11. Basu S, Nagy JA, Pal S, Vasile E, Eckelhoefer IA, Bliss VS, Manseau EJ, Dasgupta PS, Dvorak HF, Mukhopadhyay D. The neurotransmitter dopamine inhibits angiogenesis induced by vascular permeability factor/vascular endothelial growth factor. Nat Med 2001;7:569-74.

12. Bhattacharya R, Sinha S, Yang SP, Patra C, Dutta S, Wang E, Mukhopadhyay D. The neurotransmitter dopamine modulates vascular permeability in the endothelium. J Mol Signal 2008;3:14.

13. Sarkar C, Chakroborty D, Basu S. Neurotransmitters as regulators of tumor angiogenesis and immunity: the role of catecholamines. J Neuroimmune Pharmacol 2013;8:7-14.

14. Peters MA, Walenkamp AM, Kema IP, Meijer C, de Vries EG, Oosting SF. Dopamine and serotonin regulate tumor behavior by affecting angiogenesis. Drug Resist Updat 2014;17:96-104.

15. Chakroborty D, Sarkar C, Yu H, Wang J, Liu Z, Dasgupta PS, Basu S. Dopamine stabilizes tumor blood vessels by up-regulating angiopoietin 1 expression in pericytes and Kruppel-like factor-2 expression in tumor endothelial cells. Proc Natl Acad Sci USA 2011;108:20730-5.

16. Sarkar C, Chakroborty D, Dasgupta PS, Basu S. Dopamine is a safe antiangiogenic drug which can also prevent 5-fluorouracil induced neutropenia. Int J Cancer 2015;137:744-9.

17. Banerjee SK. Dopamine: an old target in a new therapy. J Cell Commun Signal 2015;9:85-6.

18. Grattan DR, Kokay IC. Prolactin: a pleiotropic neuroendocrine hormone. J Neuroendocrinol 2008;20:752-63.

19. Elias KA, Weiner RI. Direct arterial vascularization of estrogen-induced prolactin-secreting anterior pituitary tumors. Proc Natl Acad Sci USA 1984;81:4549-53.

20. Schechter J, Goldsmith P, Wilson C, Weiner R. Morphological evidence for the presence of arteries in human prolactinomas. J Clin Endocrinol Metab 1988;67:713-9.

21. Ortiz LD, Syro LV, Scheithauer BW, Ersen A, Uribe H, Fadul CE, Rotondo F, Horvath E, Kovacs K. Anti-VEGF therapy in pituitary carcinoma. Pituitary 2012;15:445-9.

22. Fedele M, Battista S, Kenyon L, Baldassarre G, Fidanza V, Klein-Szanto AJP, Parlow AF, Visone R, Pierantoni GM, Outwater E, Santoro M, Croce CM, et al. Overexpression of the HMGA2 gene in transgenic mice leads to the onset of pituitary adenomas. Oncogene 2002;21:3190-98.

23. Fedele M, De Martino I, Pivonello R, Ciarmiello A, De Caro MLDB, Visone R, Palmieri D, Pierantoni GM, Arra C, Schmid HA, Hofland L, Lombardi G, et al. SOM230, a new somatostatin analogue, is highly effective in the therapy of growth hormone/prolactin-secreting pituitary adenomas. Clin Cancer Res 2007;13:2738-44.

24. Battista S, Fidanza V, Fedele M, Klein-Szanto AJ, Outwater E, Brunner H, Santoro M, Croce CM, Fusco A. The expression of a truncated HMGI-C gene induces gigantism associated with lipomatosis. Cancer Res 1999;59:4793-7.

25. Delgrange E, Trouillas J, Maiter D, Donckier J, Tourniaire J. Sex-related difference in the growth of prolactinomas: a clinical and proliferation marker study. J Clin Endocrinol Metab 1997;82:2102-7.

26. Losa M, Mortini P, Barzaghi R, Gioia L, Giovanelli M. Surgical treatment of prolactin-secreting pituitary adenomas: early results and long-term outcome. J Clin Endocrinol Metab 2002;87:3180-6.

27. Guillou A, Romano N, Steyn F, Abitbol K, Le Tissier P, Bonnefont X, Chen C, Mollard P, Martin AO. Assessment of lactotroph axis functionality in mice: longitudinal monitoring of PRL secretion by ultrasensitive-ELISA. Endocrinology 2015;156:1924-30.

28. Chauvet N, El-Yandouzi T, Mathieu MN, Schlernitzauer A, Galibert E, Lafont C, Le Tissier P, Robinson IC, Mollard P, Coutry N. Characterization of adherens junction protein expression and localization in pituitary cell networks. J Endocrinol 2009;202:375-87.

29. Bonnefont X, Lacampagne A, Sanchez-Hormigo A, Fino E, Creff A, Mathieu MN, Smallwood S, Carmignac D, Fontanaud P, Travo P, Alonso G, Courtois-Coutry N, et al. Revealing the large-scale network organization of growth hormone-secreting cells. Proc Natl Acad Sci USA 2005;102:16880-5.

30. Lafont C, Desarmenien MG, Cassou M, Molino F, Lecoq J, Hodson D, Lacampagne A, Mennessier G, El Yandouzi T, Carmignac D, Fontanaud P, Christian H, et al. Cellular in vivo imaging reveals coordinated regulation of pituitary microcirculation and GH cell network function. Proc Natl Acad Sci USA 2010;107:4465-70.

31. Manders EMM, Verbeek FJ, Aten JA. MEASUREMENT OF COLOCALIZATION OF OBJECTS IN DUAL-COLOR CONFOCAL IMAGES. J Microscopy 1993;169:375-82.

32. Osterstock G, El Yandouzi T, Romano N, Carmignac D, Langlet F, Coutry N, Guillou A, Schaeffer M, Chauvet N, Vanacker C, Galibert E, Dehouck B, et al. Sustained alterations of hypothalamic tanycytes during posttraumatic hypopituitarism in male mice. Endocrinology 2014;155:1887-98.

33. Hashizume H, Baluk P, Morikawa S, McLean JW, Thurston G, Roberge S, Jain RK, McDonald DM. Openings between defective endothelial cells explain tumor vessel leakiness. Am J Pathol 2000;156:1363-80.

34. LeCouter J, Kowalski J, Foster J, Hass P, Zhang Z, Dillard-Telm L, Frantz G, Rangell L, DeGuzman L, Keller GA, Peale F, Gurney A, et al. Identification of an angiogenic mitogen selective for endocrine gland endothelium. Nature 2001;412:877-84.

35. Kamba T, Tam BYY, Hashizume H, Haskell A, Sennino B, Mancuso MR, Norberg SM, O'Brien SM, Davis RB, Gowen LC, Anderson KD, Thurston G, et al. VEGF-dependent plasticity of fenestrated capillaries in the normal adult microvasculature. Am J Physiol Heart Circ Physiol 2006;290:H560-H76.

36. Korsisaari N, Ross J, Wu X, Kowanetz M, Pal N, Hall L, Eastham-Anderson J, Forrest WF, Van Bruggen N, Peale FV, Ferrara N. Blocking vascular endothelial growth factor-A inhibits the growth of pituitary adenomas and lowers serum prolactin level in a mouse model of multiple endocrine neoplasia type 1. Clin Cancer Res 2008;14:249-58.

37. Hu-Lowe DD, Zou HY, Grazzini ML, Hallin ME, Wickman GR, Amundson K, Chen JH, Rewolinski DA, Yamazaki S, Wu EY, McTigue MA, Murray BW, et al. Nonclinical antiangiogenesis and antitumor activities of axitinib (AG-013736), an oral, potent, and selective inhibitor of vascular endothelial growth factor receptor tyrosine kinases 1, 2, 3. Clin Cancer Res 2008;14:7272-83.

38. Carmeliet P, Jain RK. Principles and mechanisms of vessel normalization for cancer and other angiogenic diseases. Nat Rev Drug Discov 2011;10:417-27.

39. Chakroborty D, Sarkar C, Mitra RB, Banerjee S, Dasgupta PS, Basu S. Depleted dopamine in gastric cancer tissues: dopamine treatment retards growth of gastric cancer by inhibiting angiogenesis. Clin Cancer Res 2004;10:4349-56.

40. Cristina C, Luque GM, Demarchi G, Lopez Vicchi F, Zubeldia-Brenner L, Perez Millan MI, Perrone S, Ornstein AM, Lacau-Mengido IM, Berner SI, Becu-Villalobos D. Angiogenesis in pituitary adenomas: human studies and new mutant mouse models. Int J Endocrinol 2014;2014:608497.

41. Berger M, Bergers G, Arnold B, Hammerling GJ, Ganss R. Regulator of G-protein signaling-5 induction in pericytes coincides with active vessel remodeling during neovascularization. Blood 2005;105:1094-101.

42. Aird WC. Endothelial cell heterogeneity. Cold Spring Harb Perspect Med 2012;2:a006429.

43. Hida K, Ohga N, Akiyama K, Maishi N, Hida Y. Heterogeneity of tumor endothelial cells. Cancer Sci 2013;104:1391-5.

44. Augustin HG, Koh GY, Thurston G, Alitalo K. Control of vascular morphogenesis and homeostasis through the angiopoietin-Tie system. Nat Rev Mol Cell Biol 2009;10:165-77.

45. Saharinen P, Eklund L, Pulkki K, Bono P, Alitalo K. VEGF and angiopoietin signaling in tumor angiogenesis and metastasis. Trends Mol Med 2011;17:347-62.

46. Dessapt-Baradez C, Woolf AS, White KE, Pan J, Huang JL, Hayward AA, Price KL, Kolatsi-Joannou M, Locatelli M, Diennet M, Webster Z, Smillie SJ, et al. Targeted Glomerular Angiopoietin-1 Therapy for Early Diabetic Kidney Disease. J Am Soc Nephrol 2014;25:33-42.

47. Lee J, Park D-Y, Park DY, Park I, Chang W, Nakaoka Y, Komuro I, Yoo O-J, Koh GY. Angiopoietin-1 Suppresses Choroidal Neovascularization and Vascular Leakage. Invest Ophthalmol Vis Sci 2014;55:2191-99.

48. Moreno-Smith M, Lee SJ, Lu C, Nagaraja AS, He G, Rupaimoole R, Han HD, Jennings NB, Roh JW, Nishimura M, Kang Y, Allen JK, et al. Biologic effects of dopamine on tumor vasculature in ovarian carcinoma. Neoplasia 2013;15:502-10.

49. Hoeppner LH, Wang Y, Sharma A, Javeed N, Van Keulen VP, Wang E, Yang P, Roden AC, Peikert T, Molina JR, Mukhopadhyay D. Dopamine D2 receptor agonists inhibit lung cancer progression by reducing angiogenesis and tumor infiltrating myeloid derived suppressor cells. Mol Onc 2015;9:270-81.

50. O'Hayre M, Degese MS, Gutkind JS. Novel insights into G protein and G protein-coupled receptor signaling in cancer. Curr Opin Cell Biol 2014;27:126-35.

Figure Legends

Figure 1: Aberrant growth of blood vessels in Hmga2/T tumors.

(A and B) Representative sections of pituitary from WT (A) and pituitary tumors from Hmga2/T (B) mice immunostained with endomucin, a marker of blood vessels. Vascular density was lower in tumors and tumoral blood vessels were structurally altered, exhibiting dilation and strong tortuosity (arrows). Extravasation of red blood cells was present in tumors (double arrows). Scale bar: 50 μm. (C-G) Blood vessels visualized by SEM in pituitary sections from WT (C) and Hmga2/T mice (D-G). Vessels were enlarged and disorganized in tumors (D and F). Endothelial cells in tumor vessels overlapped one another with abnormal connections (E, arrows). (G) Higher magnification of F showing endothelial cells protruding

into the lumen (asterisk). Scale bar: 5 μm in C; 10 μm in D-G. (H-J) Ultrastructural visualization of blood vessels by transmission electron microscopy in pituitary from WT (H) and Hmga2/T mice (I and J). A capillary from normal pituitary, surrounded by endocrine cells, displayed a regular and smooth endothelium, a perivascular space with collagen fibers. By contrast, in tumors, vessels were large and disorganized. The endothelium was damaged, protrusions into the lumen were observed (arrows, I), and numerous red blood cells were present outside the vessels (asterisks, I and J). Scale bar: 5 μm in H-J. (K and L) *In vivo* imaging of pituitaries from WT (K) and Hmga2/T (L) mice after iv injection of fluorescent labeled-dextran. In WT, fluorescence was first detected in dural arteries from meninges surrounding the pituitary (arrows). Fluorescence was present in the adenohypophysis after 4 s and the whole pituitary vasculature was filled after 24 s. In Hmga2/T mice, in the tumoral region, the fluorescence was observed in vessels derived from dural arteries (arrowheads). Note that detection of fluorescence in the adenohypophysis through the portal system started at 21 s. Filling of the portal capillaries was complete after 1 min and 49 s. Letters C and R indicate the caudal-rostral orientation of the animal.

Figure 2: The direct arterial blood supply in tumors impedes the dopaminergic inhibitory tone without major hypothalamic dysfunction.

(A) Dopaminergic inhibitory tone in WT and Hmga2/T mice at various stages. PRL blood concentrations were measured in basal conditions and after an injection of the D2R antagonist domperidone. The DA inhibitory tone (ratio between maximal and basal PRL secretion ± sem) was high in wild-type mice and during hyperplasia while tumors displayed a significantly lower tone. WT: n = 7; Hyperplasia: n = 7; Tumors 7-20 mg: n = 6; Tumors >20mg: n = 8. (B) Confocal images showing immunofluorescence labeling of hypothalamus sections from WT (left) and Hmga2/T mice (right) with TH (top) and phosphorylated TH

(pTH, bottom) antibodies. The staining obtained with TH or pTH antibody was similar in the arcuate nucleus and median eminence region in WT and Hmga2/T mice, showing that TIDA neurons were present and still produced DA in animals harboring tumors. Scale bar: 100 μm. (C) Amperometric measurements of DA secretion in the median eminence *in vivo* before the onset of tumors and during tumoral progression assessed by PRL concentration in blood.

Figure 3: Bromocriptine prevents tumoral progression, aberrant vascular supply, and restores angiogenic balance.

(A) Photographs of pituitary adenomas from Hmga2/T mice with (Bromocriptine 6 wks) and without (Tumor 6 wks) treatment with bromocriptine implants for 6 weeks, compared to pituitary tumor at the beginning of the treatment (Tumor t0). Scale bar: 2 mm. (B) Weight of pituitaries from Hmga2/T mice at the beginning of the treatment (Tumors t0, n = 6), or receiving or not (Tumors 6 wks, n = 6) bromocriptine for 6 weeks (Bromocriptine 6 wks, n = 5). Tumoral progression was inhibited by bromocriptine. Kruskal-Wallis test followed by Dunn's multiple comparisons test, ** $P<0.01$. (C) Quantification of microspheres present in the adenohypophysis of Hmga2/T mice at the beginning of the treatment, or receiving or not bromocriptine for 6 weeks. The number of microspheres was significantly lower in bromocriptine-treated mice (n = 5) compared to untreated mice (n = 6). Kruskal-Wallis test followed by Dunn's multiple comparisons test, *** $P<0.001$. (D) Expression of pro- and anti-angiogenic factors in tumoral Hmga2/T compared to WT mice. Angiogenic factor mRNA levels were quantified in Hmga2/T mice harboring pituitary tumors (n = 7) and WT of similar age (n = 5) by qPCR. Angiogenic profiles were altered in pituitary adenomas. Mann-Whitney test, * $P<0.05$, ** $P<0.01$. (E) Long-term effects of bromocriptine on angiogenic profiles in pituitary tumors. Angiogenic factor mRNA levels were quantified by qPCR in Hmga2/T mice harboring pituitary tumors and treated (n = 4) or not (n = 7) with implants of bromocriptine

for 6 weeks. Results are presented as ratio of gene expression in bromocriptine-treated tumors to untreated-tumors and show that bromocriptine restored the expression of angiogenic factors in tumors. Mann-Whitney test, * P<0.05, ** P<0.01. (F) *Angpt1*, *Prok1* and *Vegfa* mRNA expression in pituitaries from Hmga2/T mice harboring tumors that received an acute treatment with bromocriptine (n = 5) or vehicle (n = 5). While *Vegfa* expression was not modified by bromocriptine, the D2R agonist increased *Angpt1* and *Prok1* mRNA levels. Mann-Whitney test, * P<0.05.

Figure 4: Involvement of Vegf in the establishment of aberrant blood supply and tumor growth.

(A) Photographs of pituitary adenomas from Hmga2/T mice treated after tumor onset for 6 weeks with vehicle or the anti-angiogenic agent axitinib. Axitinib-treated tumors appeared less hemorrhagic and tumor growth was reduced. (B) Weight of pituitaries from Hmga2/T mice receiving vehicle or axitinib for 6 weeks. Tumoral growth was decreased by axitinib. Mann Whitney test, ** P<0.01. (C) Quantification of microspheres present in the adenohypophysis from Hmga2/T mice receiving vehicle or axitinib for 6 weeks. The number of microspheres was significantly lower in axitinib-treated mice (n = 5) compared to vehicle-treated mice (n = 6). Mann Whitney test, ** P<0.01. (D) Long-term effects of axitinib on angiogenic profiles in pituitary tumors. Angiogenic factor mRNA levels were quantified by qPCR in Hmga2/T mice harboring pituitary tumors and treated (n = 4) or not (n = 6) with axitinib for 6 weeks. Results are presented as ratio of gene expression in axitinib-treated tumors to untreated-tumors and show that axitinib did not restore the expression of *Angpt1* and *Prok1* in tumors. Mann-Whitney test, * P<0.05, ** P<0.01.

Figure 5: Complementary effects of bromocriptine and axitinib on intratumoral hemorrhage.

(A) Photographs of pituitary adenomas from Hmga2/T mice harboring untreated-tumors, or tumors treated for 6 weeks with either bromocriptine or axitinib, or combined bromocriptine and axitinib. (B) Paraffin embedded pituitary sections from WT mice, hyperplastic Hmga2/T mice, and Hmga2/T mice with pituitary tumors receiving various treatments for 6 weeks. Tissue sections were immunostained with endomucin, a marker of blood vessels. Scale bar: 50 μm. Arrows: blood lakes. To better illustrate vascular density and defects, corresponding binary images obtained for quantification of blood vessel structural parameters are shown. (C) Ultra-structural visualization of pituitary blood vessels by TEM from WT and Hmga2/T mice exhibiting untreated-tumors, or tumors treated for 6 weeks with various therapies. Scale bar: 5 μm. (D) Quantification of extravasation area in pituitary sections from WT and Hmga2/T mice receiving various treatments. Combination treatment with bromocriptine and axitinib almost totally abolished intratumoral hemorrhage. n = 4 mice per condition. Kruskal-Wallis test followed by Dunn's multiple comparisons test, * $P<0.05$, ** $P<0.01$, *** $P<0.001$.

Figure 6: Restoration of blood vessel perfusion by bromocriptine and axitinib combination treatment.

(A) Blood vessel perfusion was assessed by intravenous injection of FITC-dextran in WT and Hmga2/T mice receiving various treatments. Pituitary sections were stained with endomucin (red) to visualize microvasculature. Poorly perfused blood vessels appeared in red and are particularly numerous in images obtained from untreated tumors. By contrast, the majority of blood vessels from tumors treated with both bromocriptine and axitinib exhibited green fluorescence. Scale bar: 200 μm. (B) Quantification of the overlap coefficient M1 reflecting the fraction of blood vessels filled with FITC-dextran in WT and Hmga2/T mice.

Combination treatment with bromocriptine and axitinib restored blood vessel perfusion, which was strongly impaired in untreated tumors, more effectively than each therapy alone. n = 4 mice per condition. Kruskal-Wallis test followed by Dunn's multiple comparisons test, *** $P<0.001$.

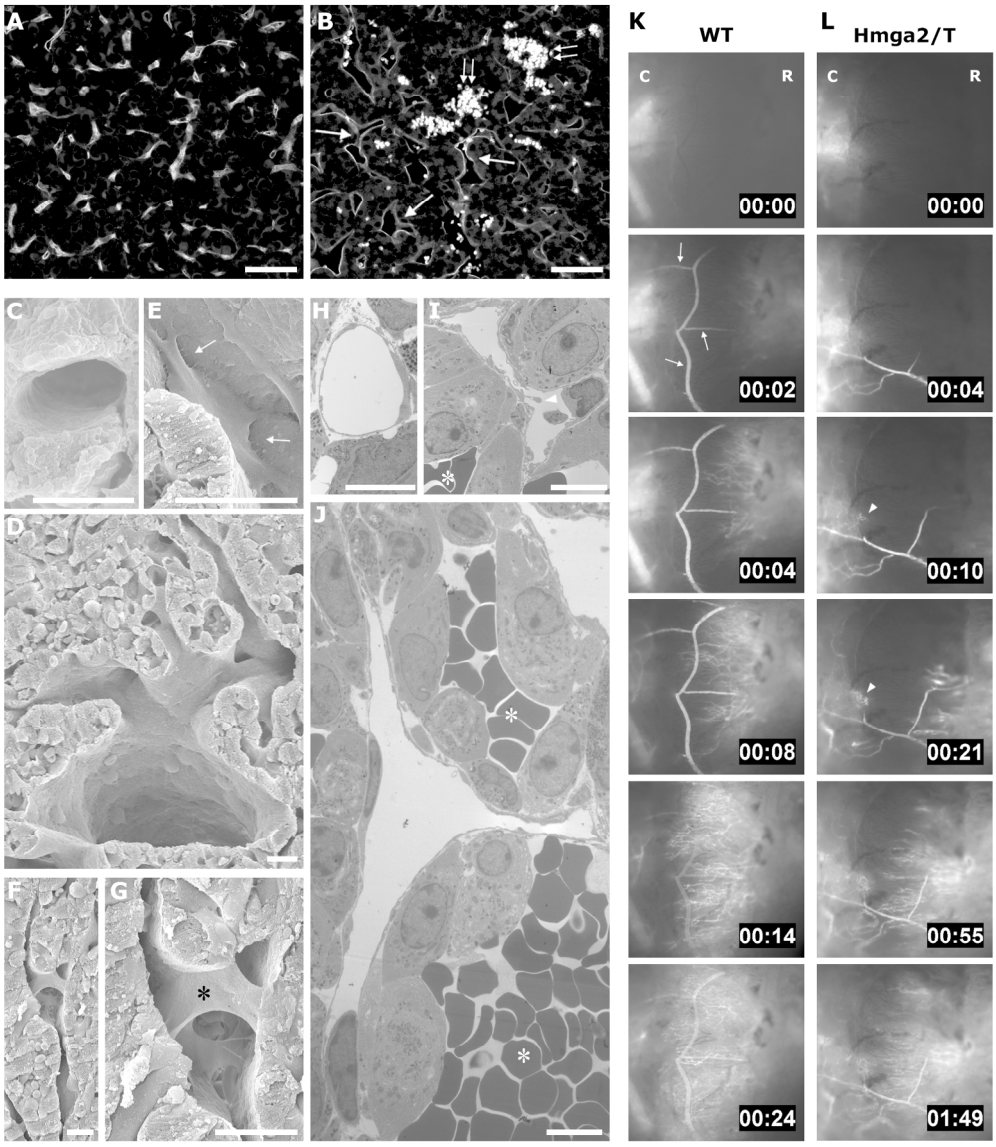

Figure 1: Aberrant growth of blood vessels in Hmga2/T tumors.
Figure 1
184x213mm (300 x 300 DPI)

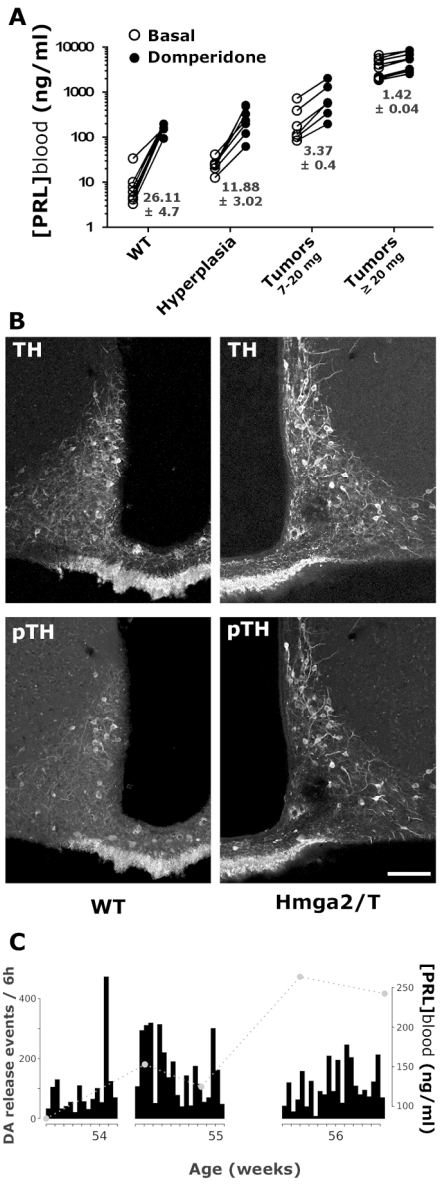

Figure 2: The direct arterial blood supply in tumors impedes the dopaminergic inhibitory tone without major hypothalamic dysfunction.
Figure 2
79x214mm (300 x 300 DPI)

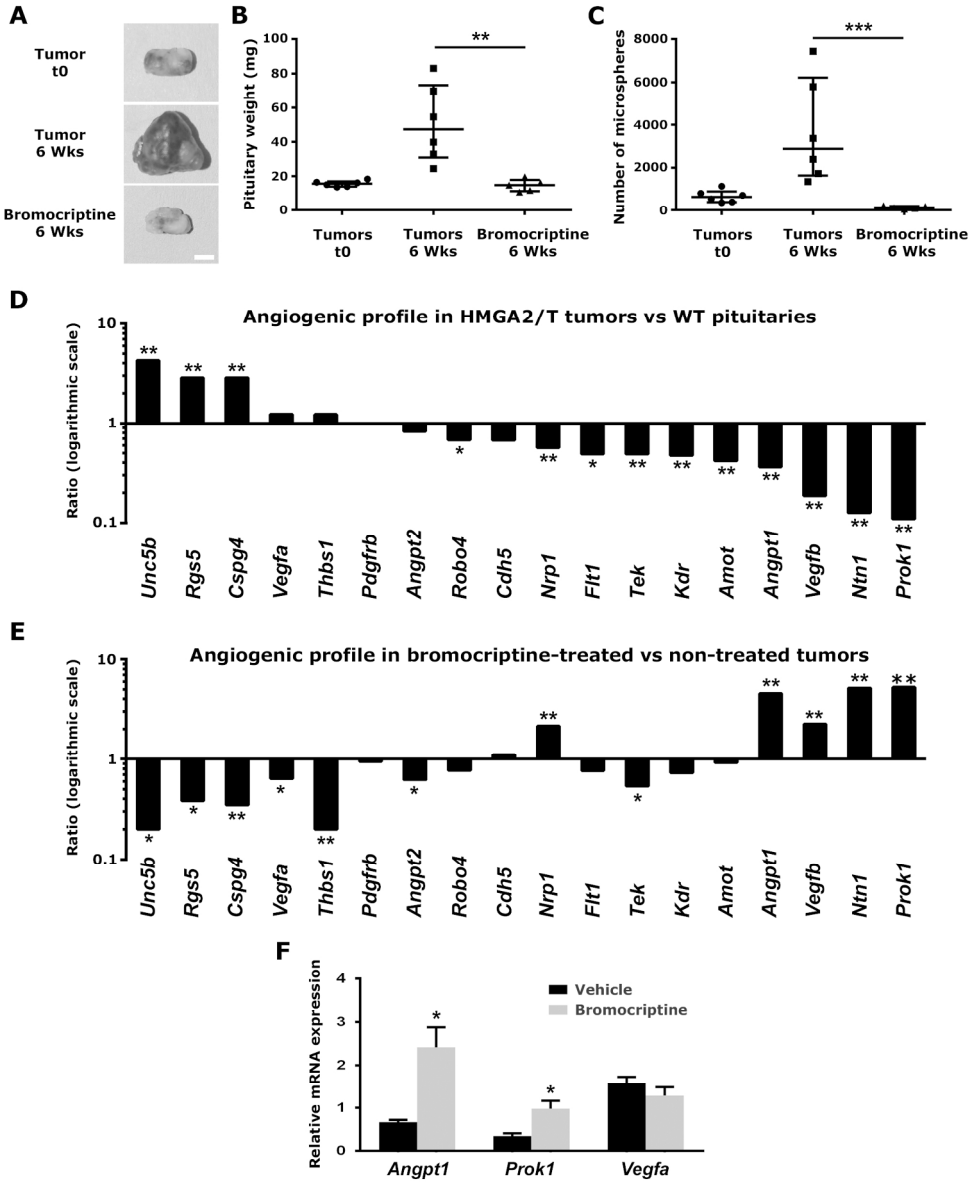

Figure 3: Bromocriptine prevents tumoral progression, aberrant vascular supply, and restores angiogenic balance.
Figure 3
170x209mm (300 x 300 DPI)

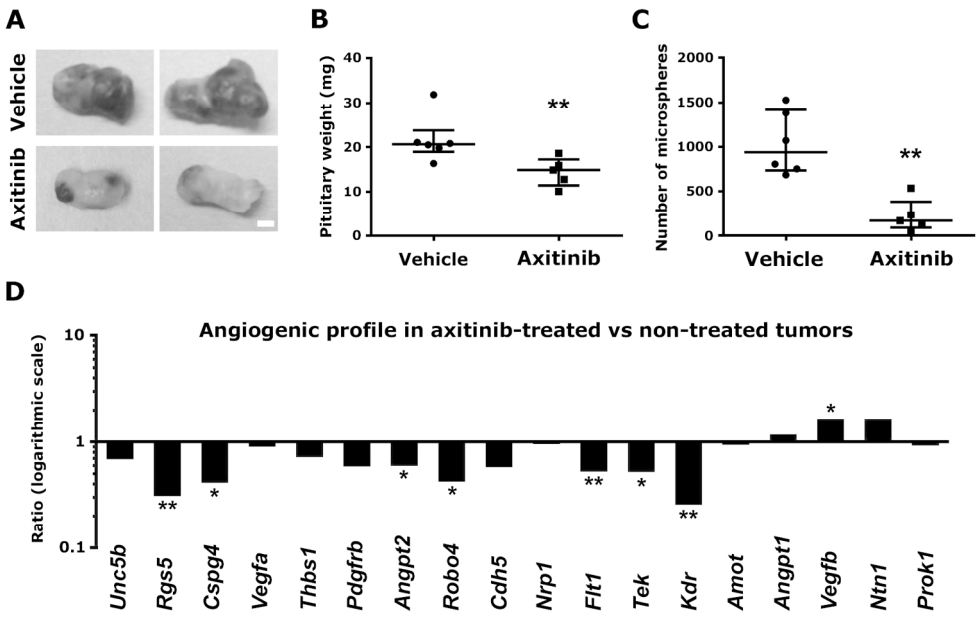

Figure 4: Involvement of Vegf in the establishment of aberrant blood supply and tumor growth.
Figure 4
163x102mm (300 x 300 DPI)

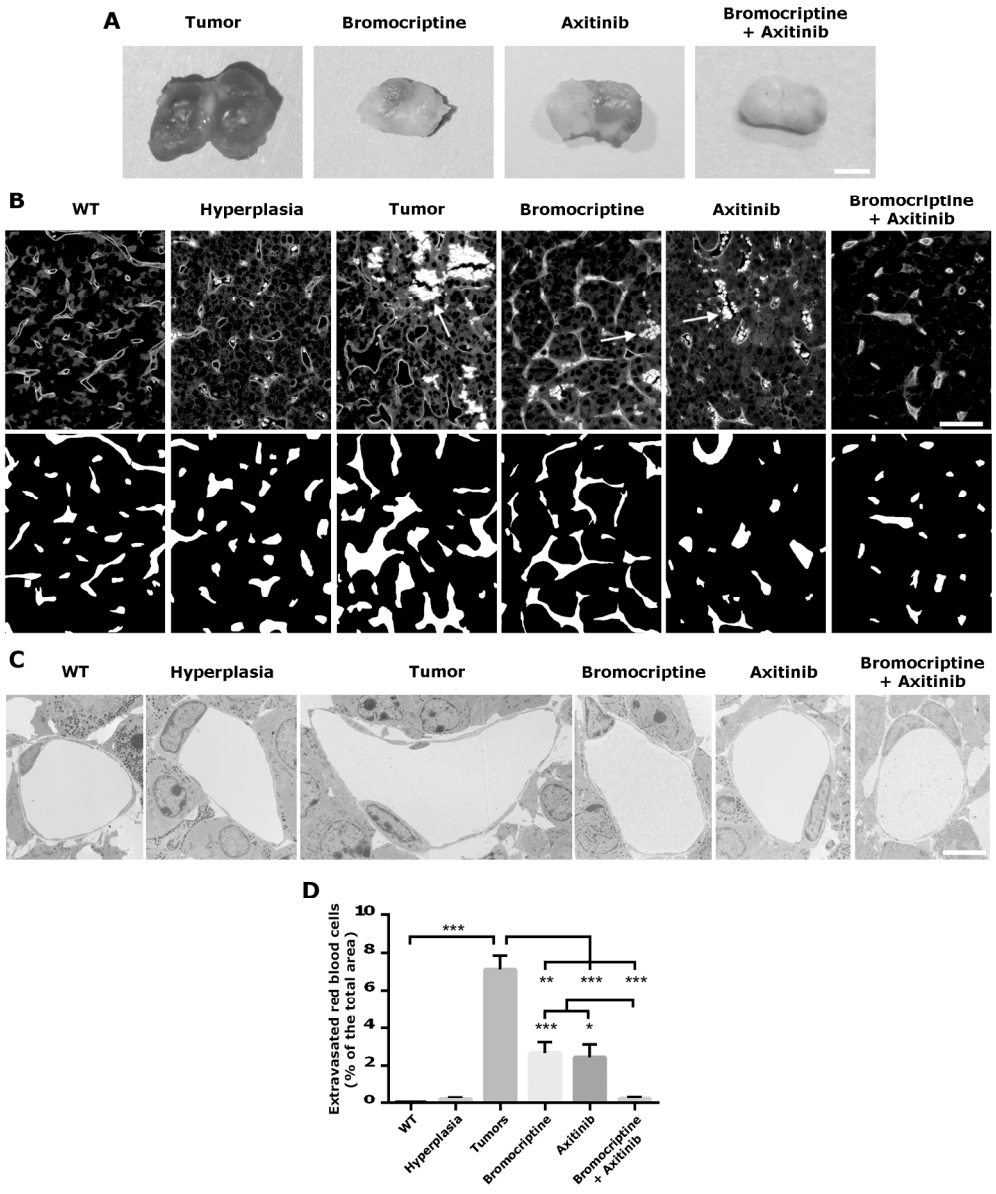

Figure 5: Complementary effects of bromocriptine and axitinib on intratumoral hemorrhage.
Figure 5
184x222mm (300 x 300 DPI)

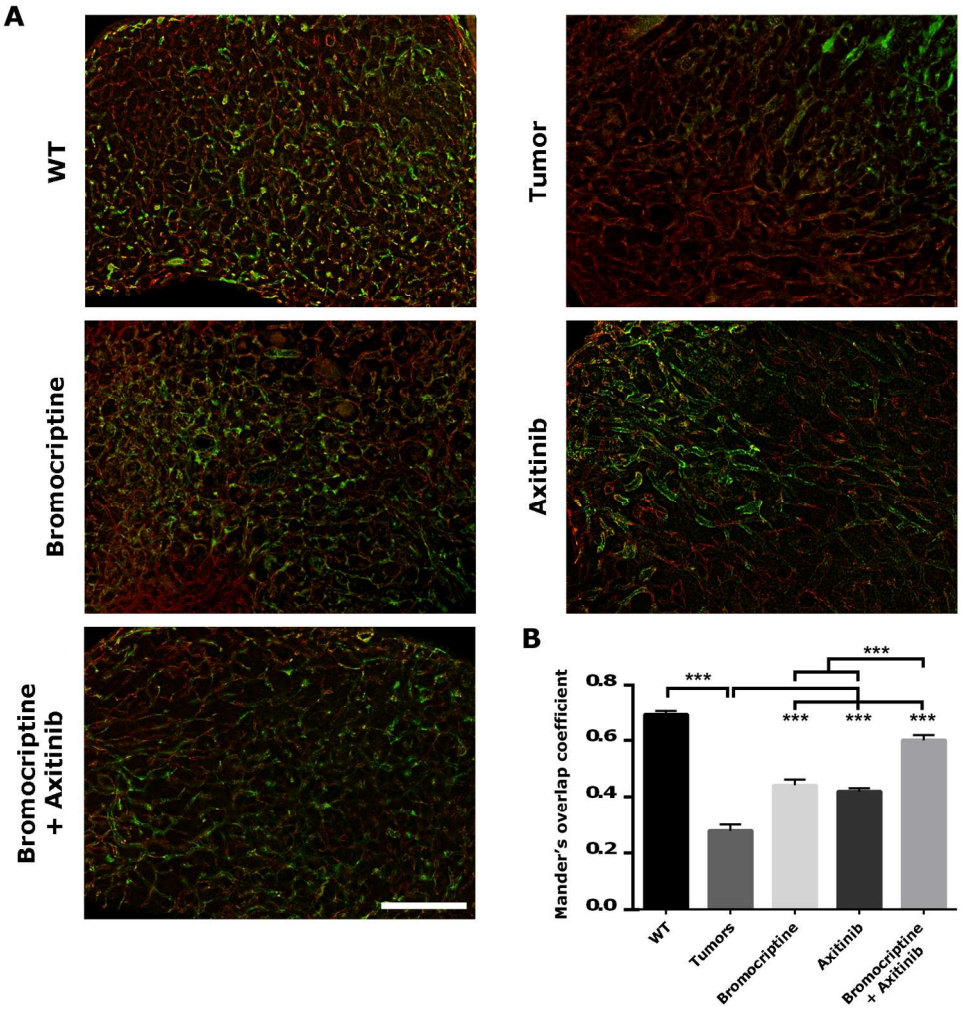

Figure 6: Restoration of blood vessel perfusion by bromocriptine and axitinib combination treatment.
Figure 6
156x159mm (300 x 300 DPI)